

Application of piezoelectric macro-fiber-composite actuators to the suppression of noise transmission through curved glass plates

Kateřina Nováková,^{1,2,*} Pavel Mokřý,¹ and Jan Václavík²

¹*Institute of Mechatronics and Computer Engineering,*

Technical University of Liberec, CZ-46117 Liberec, Czech Republic

²*Research Centre for Special Optics and Optoelectronic Systems (TOPTEC),*

Sobotecká 1660, CZ-51101 Turnov, Czech Republic

(Dated: December 3, 2024)

Abstract

The possibility of increasing the acoustic transmission loss of sound transmitted through planar or curved glass shells using attached piezoelectric Macro Fiber Composite (MFC) actuators shunted by active circuits with a negative capacitance is analyzed. The key features that control the sound transmission through the curved glass shells are analyzed using an analytical approximative model. The detailed analysis of the particular arrangement of MFC actuators on the glass shell is performed using a Finite Element Method (FEM) model. The FEM model takes into account the effect of a flexible frame that clamps the glass shell at its edges. The method for the active control of the Young's modulus and the bending stiffness coefficient of the composite sandwich structure that consists of a glass plate and the attached piezoelectric MFC actuator is presented. The predictions of the acoustic transmission loss frequency dependencies obtained by the FEM model are compared with experimental data. The results indicate that it is possible to increase the acoustic transmission loss by 20 dB and 25 dB at the frequencies of the first and second resonant modes of the planar and curved glass shells, respectively, using the effect of the shunt circuit with a negative capacitance.

Keywords: Glass window, MFC piezoelectric actuator, Noise Transmission, FEM Simulation

*Electronic address: katerina.novakova3@tul.cz

I. INTRODUCTION

Windows and glazed facades often represent a major paths that transmit the noise to the building interior. The noise intensity in cities is steadily increasing. Unfortunately, the passive noise control methods are often not efficient, especially in the low frequency range (up to 1 kHz). In addition, they can be problematically applicable in the case of large glazed windows or facades. At the same time, it is difficult to find a realization of the active noise control that would be both efficient in the broad frequency range and financially acceptable. All in all, the control of noise transmission through large planar plates has become a challenge for scientists and technicians in the field of acoustics.

The most common methods of passive noise control are based on the laminated glass technology and double glazing (see e.g. [1]). Laminated glass with the different thicknesses of interlayer and glass can improve the acoustical performance by reducing the noise transmission in the fenestration system. Double glazed windows use two separate panels of glass with an air space between them. Such a double structure has a resonance frequency, which depends on the mass and distance of the plates, and on the stiffness of the cavity medium. At the resonance frequency, the sound insulation is minimal. Above the resonance frequency, the sound proofing capability rises three times faster than below the resonance. The both aforementioned methods are efficient in reducing the noise transmission at frequencies higher than 1.5 kHz. On the other hand, acoustic performance of the double glazed window deteriorates rapidly below the double structures resonance, where its acoustic shielding can be even worse than that of a single glass plate. Anyway, in order to achieve a reasonable low-frequency noise transmission suppression, heavy structures are required, which leads to significant weight penalties. As a result, the search for alternative ways of the low-frequency noise transmission suppression has become a very important research area.

The active noise control (ANC), in which secondary waves interfere destructively with the disturbing noise, was used for the attenuation of sound transmission through aluminum elastic plates in the works by Fuller et al. [2, 3]. The performance of the active system in reducing the transmitted sound was tested for several input frequencies up to 200 Hz and the reduction of about 15 – 25 dB in a sound transmission was achieved. Piezoelectric actuators have been investigated for use as active control inputs in [4]. These results show that a reduction of sound transmission through the plate can be successfully achieved, if the

proper size, number and position of the piezoelectric actuators are chosen. A recent work by Zhu [5] shows the development of thin glass panels, whose vibrations can be controlled electronically by small rare earth voice coil actuators. The development of the control system is based on the use of a wave separation algorithm that separates the incident sound from the reflected sound. Using this method, the sound transmission reduction by 10 – 15 dB in a broadband frequency range up to 600 Hz was achieved. ANC was also used to improve the sound insulation of double-glazed windows. Jakob and Möser obtained their results with a feedforward [6] and adaptive feedback controller [7]. They presented a comprehensive overview of the system with various numbers and positions of loudspeakers and microphones inside the cavity and they gave some insight into the physics of the active double-glazed window. The total sound pressure level can be reduced by nearly 8 dB and somewhat more than 5 dB with feedforward and feedback control, respectively, in the frequency range up to 400 Hz.

Later, the Active Structural Acoustic Control (ASAC) method has been developed for the reduction of the structure-borne noise. In this method, vibrating structures are used as secondary noise sources to suppress sound fields generated by primary noise sources from outside (see e.g. Pan et al [8, 9], Hirsch et al. [10]). Various studies use the properties of passive double panel system to enhance the noise control performance (e.g. Carneal et al. [11]). Naticchia and Carbonari studied the implementation of an active structural control system for glazed facades [12]. They obtained a sound reduction of the highest value up to 15 dB in the low frequency range (up to 200 Hz). They have also proposed a procedure to combine this approach with the laminated glass plates, which are more effective at higher frequencies. However, when applied to building windows, ANC method requires external microphones for the disturbance monitoring, and internal error sensors and loudspeakers for the control purposes. In order to develop model-based ASAC schemes, a good understanding of structural–acoustic interactions in the considered system is required. Both of these methods require a fast control algorithm and powerful electronics. In general, such requirements yield rather expensive and energy consuming systems.

The third category of noise suppression methods is based on the semi-active control approach. An example to be mentioned here is the possibility of the arrangement of optimally tuned Helmholtz resonators (HRs) that result in an increase in the acoustical damping level inside the cavity between the double plates. The HR is one of the most common devices for

passive control of noise at low frequencies. Mao and Pietrzko [13] developed a fully coupled system of structural-acoustic-HRs for the double wall structures by the modal coupling method. The simulations were confirmed by their experimental work [14]. With optimally tuned HRs it is possible to achieve the sound reduction up to 18 dB at certain low frequencies (to 100 Hz). Recent results concerning the active and passive control of sound transmission through double wall structures have been summarized in the review by Pietrzko and Mao. [15].

Another example of the semi-active noise cancellation method with a rather high application potential is the Piezoelectric Shunt Damping (PSD). This method uses electro-acoustic transducers connected to a passive or an active shunt circuit. The approach with passive shunt circuits has been studied by Fleming et. al (see e.g. [16–18]). It is mainly focused on narrow frequency band devices (based on passive RL shunts) and relatively complicated control algorithms based on classical Linear Quadratic Gaussian methods (LQG) implemented through digital signal processors. Recently, reduction of noise transmission through a stiffened panel by 16 dB in the low-frequency range around the first resonance has been demonstrated by Yuan et al. [19]. In this work, the results have been obtained using hybrid control strategy combining the feedforward and feedback control. The same value of noise transmission suppression have attained by Ciminello et al. [20] using a 6-PZT network multi-tone Switching Shunt Control (SSC) system embedded into a balanced fiberglass laminate.

In this Article, we have focused on the Active Piezoelectric Shunt Damping (APSD) that offers an attractive approach for reduction of the noise level transmitted through windows in buildings. The APSD method is based on the change of the vibrational response of the structure using piezoelectric actuators shunted by electronic circuits that have a negative effective capacitance. It was shown by Date et al. [21] that the effective value of Young’s modulus can be controlled to a large extent (from 0 to infinity) using the negative capacitor shunt. With use of this active elasticity control, resonant frequencies of the noise suppression system can be redistributed in such a way that the noise transmission through the system is greatly reduced. This approach combines the advantages of both passive and active noise control methods and it has been applied in several systems for the vibration transmission suppression [22–25]. Advantages of the APSD method stem from realization of inexpensive devices that are efficient in a wide frequency range (e.g. from 10 Hz to 100 kHz [26]) and

with a low electric energy consumption [27].

The objective of this study is to analyze the most efficient ways for suppression of noise transmission through the glass plates using active elasticity control of attached piezoelectric elements. To achieve this objective, the physical quantity called acoustic transmission loss (TL) that measures the noise transmission through glass plates is introduced in Sec. II. The most important features of the noise transmission through glass plates are analyzed using the approximative analytical model presented in Sec. III. In Sec. IV, there are presented the key aspects of the application of the active elasticity control to the noise transmission suppression through composite structures with piezoelectric layers. In order to verify the applicability of the APSD method to the noise transmission suppression through the glass plates, the Finite Element Method (FEM) simulations of the sound transmission through the glass plate with that attached piezoelectric elements shunted with negative capacitance circuits is used. Section V presents details of the FEM model implementation including calculation of the effective Young's modulus of the piezoelectric Macro Fiber Composite (MFC) actuator, calculation of the acoustic transmission loss and the role of the boundary condition on its frequency dependence. Section VI describes a simple experimental setup for the approximative measurements of the acoustic transmission loss. Results of the FEM model simulations and their comparison with experimental data are presented in Sec. VII. Finally, numerical simulations and experimental results are discussed in Sec. VIII.

II. ACOUSTIC TRANSMISSION LOSS OF THE GLASS PLATE

The sound shielding efficiency of the window is measured by the physical quantity called *Acoustic Transmission Loss* (TL). Let us consider a simple system shown in Fig. 1(a). The system consists of a glass plate fixed in a rigid frame at its edges. The sound source located underneath the glass plate generates an incident sound wave of the acoustic pressure p_i that strikes the glass plate. It makes the glass plate vibrate, so that a part of the sound wave is reflected and a part is transmitted with the values of the acoustic pressures p_r and p_t , respectively. The value of TL is defined as a ratio, usually expressed in decibel scale, of the acoustic powers of the incident and transmitted acoustic waves, respectively.

$$TL = 20 \log_{10} \left| \frac{p_i}{p_t} \right|. \quad (1)$$

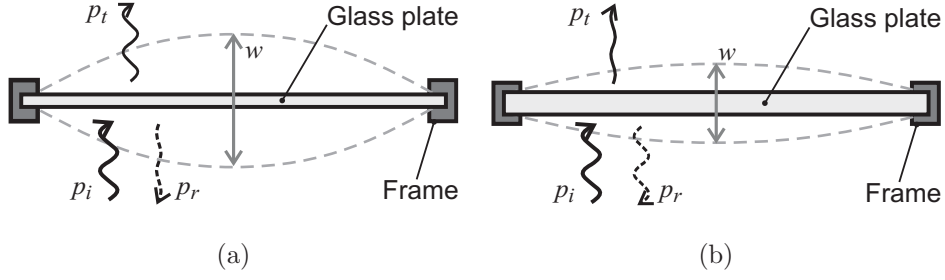


Figure 1: (a) Scheme of the considered sound transmission system, which consists of the glass plate fixed in a rigid frame at its edges. The sound source located underneath the glass plate generates an incident sound wave of the acoustic pressure p_i that strikes the glass plate. It makes the glass plate vibrate and a part of the sound wave is reflected and a part is transmitted with the values of the acoustic pressures p_r and p_t , respectively. The dashed line indicates the vibration amplitude of the glass plate (for simplicity - first mode of vibration); (b) Scheme of the noise suppression principle: When the vibration amplitude normal to the surface of the glass plate is reduced (e.g. due to being thicker), the greater part of the incident sound wave energy is reflected than transmitted.

The value of TL can be expressed in terms of the specific acoustic impedance of the window Z_w as it was presented in [28]:

$$TL = 20 \log_{10} \left| 1 + \frac{Z_w}{2Z_a} \right|, \quad (2)$$

where $Z_a = \rho_0 c$ is the specific acoustic impedance of air, ρ_0 is the air density and c is the sound velocity in the air. The specific acoustic impedance of the glass plate is defined by the formula:

$$Z_w = \Delta p / v, \quad (3)$$

where v and $\Delta p = (p_i + p_r) - p_t$ are the normal component of vibration velocity and the acoustic pressure difference at the opposite sides of the glass plate, respectively.

Figure 1(b) presents a scheme of the noise suppression principle that follows from Eqs. (2) and (3), i.e., the values of specific acoustic impedance Z_w and acoustic transmission loss TL increase with a decrease in the amplitude of the window vibration velocity v . In order to optimize the system and to achieve maximum values of TL , it is necessary to understand the dynamics and vibrational response of the glass plate.

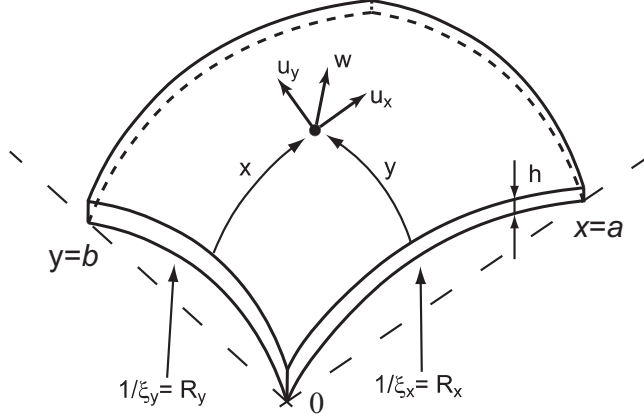


Figure 2: Geometry of the rectangular-like curved glass shell of constant thickness h . Symbols x and y stand for curvilinear orthogonal coordinates. The shell dimensions are denoted by symbols a and b . The shell has constant radii of curvatures along the x and y coordinates denoted by symbols $R_x = 1/\xi_x$ and $R_y = 1/\xi_y$. Symbols u_x and u_y stand for tangential components of the displacement of the infinitesimal shell element. The symbol w stands for the normal component of the displacement of the shell element.

III. ANALYTICAL ESTIMATION OF THE ACOUSTIC IMPEDANCE OF A CURVED GLASS SHELL

In order to determine the parameters of the glass plate that control its vibrational response, the analytical model of the vibration of generally curved glass shells is developed in this Section. For simplicity, consider a rectangular-like glass shell of a constant thickness h and with the dimensions denoted by symbols a and b , which is shown in Fig. 2. Consider a curvilinear orthogonal coordinates x and y , that define the position on the curved surface of the shell. Consider that the shell has constant radii of curvature along the x and y coordinates denoted by symbols R_x and R_y , respectively. It is convenient to introduce the symbols $\xi_x = 1/R_x$ and $\xi_y = 1/R_y$ for local curvatures of the shell along the x and y directions, respectively. Symbols u_x and u_y stand for tangential components of the displacement of the infinitesimal shell element with the volume $h dx dy$. The symbol w stands for the normal component of the displacement of the shell element.

Using the fundamental equations presented in basic textbooks [29–31], i.e. equations expressing: (i) equilibrium of forces and moments acting on an infinitesimal shell element,

(ii) the Hooke's law, and (iii) the relations between the components of the strain tensor and the shell displacements u_x , u_y , and w ; it is a relatively straightforward task to arrive at the following equations of motion:

$$Yh \left[\frac{1}{2(1-\nu^2)} \frac{\partial^2 u_x}{\partial x^2} + \frac{1}{2(1+\nu)} \frac{\partial^2 u_x}{\partial y^2} - \frac{1}{2(1-\nu)} \frac{\partial^2 u_y}{\partial x \partial y} - \frac{\xi_x + \nu \xi_y}{2(1-\nu^2)} \frac{\partial w}{\partial x} \right] = \varrho h \frac{\partial^2 u_x}{\partial t^2}, \quad (4a)$$

$$Yh \left[\frac{1}{2(1+\nu)} \frac{\partial^2 u_y}{\partial x^2} + \frac{1}{2(1-\nu^2)} \frac{\partial^2 u_y}{\partial y^2} - \frac{1}{2(1-\nu)} \frac{\partial^2 u_x}{\partial x \partial y} - \frac{\nu \xi_x + \xi_y}{2(1-\nu^2)} \frac{\partial w}{\partial y} \right] = \varrho h \frac{\partial^2 u_y}{\partial t^2}, \quad (4b)$$

$$-G\Delta^2 w + \Delta p + \frac{Yh}{1-\nu^2} \left[(\xi_x + \nu \xi_y) \frac{\partial u_x}{\partial x} + (\nu \xi_x + \xi_y) \frac{\partial u_y}{\partial y} - (\xi_x^2 + \xi_y^2 + 2\nu \xi_x \xi_y) w \right] = \varrho h \frac{\partial^2 w}{\partial t^2}, \quad (4c)$$

where

$$\Delta^2 w = \frac{\partial^4 w}{\partial x^4} + 2 \frac{\partial^4 w}{\partial x^2 \partial y^2} + \frac{\partial^4 w}{\partial y^4} \quad (5)$$

is the biharmonic operator. The symbol G stands for the bending stiffness coefficient, the symbol Y stands for the Young's modulus, ϱ is the mass density of the material and ν is its Poisson's ratio. The symbol Δp stands for the difference of the acoustic pressures at the opposite sides of the curved shell and represents the "driving force" of the system.

It is seen that the first and second equations in Eqs. (4) represent the equations of motion for the tangential components u_x and u_y of the shell displacement. These are coupled with the normal component of the shell displacement w and the driving force Δp via the nonzero values of curvatures ξ_x and ξ_y . It can be shown that for relatively small numerical values of curvatures considered in this work, the values of all terms, which contain the tangential components u_x and u_y in Eq. (4c), are much smaller than the remaining terms with the normal component w of the displacement. Under this consideration, the system of Eqs. (4) can be further reduced down to a single partial differential equation in a form:

$$-G \left(\frac{\partial^4 w}{\partial x^4} + 2 \frac{\partial^4 w}{\partial x^2 \partial y^2} + \frac{\partial^4 w}{\partial y^4} \right) + \frac{Yh}{1-\nu^2} (\xi_x^2 + \xi_y^2 + 2\nu \xi_x \xi_y) w + \Delta p = \varrho h \frac{\partial^2 w}{\partial t^2}. \quad (6)$$

When one considers a simple situation: (i) the shell is formed by a rectangular part of a spherical shell, i.e. $\xi_x = \xi_y = \xi$, (ii) the steady state, when the shell is driven by the pure tone of angular frequency ω , i.e. $\Delta p(t) = P e^{i\omega t}$ and $w(x, y, t) = w(x, y) e^{i\omega t}$, and (iii) the boundary conditions of the simple supported shell, i.e. $w(0, y) = w(a, y) = w_{xx}(0, y) = w_{xx}(a, y) = 0$ and $w(x, 0) = w(x, b) = w_{yy}(x, 0) = w_{yy}(x, b) = 0$, the solution of the

partial differential equation Eq. (5) can be easily found in the form of Fourier series:

$$w(x, y, t) = \sum_{n,m=1}^{\infty} \frac{16P(1-\nu) \sin[(2n-1)\pi x/a] \sin[(2m-1)\pi y/b] e^{i\omega t}}{(2n-1)(2m-1)\pi^2 \{2Yh\xi^2 + (1-\nu)[G((2m-1)^2/b^2 + (2n-1)^2/a^2) - \rho h\omega^2]\}}. \quad (7)$$

Now, the effective value of the specific acoustic impedance Z_w can be expressed in the following form:

$$Z_w(\omega) \approx \Delta p(0) \left[i\omega \sqrt{\frac{1}{ab} \int_a^0 dx \int_b^0 w(x, y, 0)^2 dy} \right]^{-1}. \quad (8)$$

When we substitute the expression for the normal displacement of the spherical shell w from Eq. (7), one can arrive at the following formula for the effective specific acoustic impedance:

$$Z_w(\omega) \approx \left\{ \sum_{n,m=1}^{\infty} \left[\frac{8i\omega a^2 b^2 (1-\nu)}{(2m-1)(2n-1)\pi^2 (G\zeta_{mn} + 2Yh\xi^2 - (1-\nu)\rho h\omega^2)} \right]^2 \right\}^{-1/2}, \quad (9)$$

where

$$\zeta_{mn} = \pi^4 (1-\nu)^2 (1+\nu) [(2m-1)^2/b^2 + (2n-1)^2/a^2]^2.$$

It is clear that Eq. (7) describes the displacement of the rectangular part of a spherical shell in a special situation without much practical interest. On the other hand, the presented analytical solution serves a possibility to trace the key features of the system that can be used for the suppression of the noise transmission.

First, it is seen that with an increase of the glass shell curvature ξ , the term $2Yh\xi^2$ in the denominator of Eq. (7) increases. This yields the decrease of the amplitude of the shell displacement and, therefore, the decrease of the normal velocity of vibrations. As a result, the value of the specific acoustic impedance of the glass shell Z_w increases with an increase in its curvature ξ as it can be seen in Eq. 9. The reason for this curvature effect is that the normal displacement of the curved shell is controlled by the in-plane stiffness, in addition to the bending flexural rigidity. Second, the specific acoustic impedance Z_w of the curved shell, i.e. $\xi > 0$, increases with an increase in the Young's modulus Y . Third, the value of Z_w of the plane plate, i.e. $\xi = 0$, increases with an increase in the bending stiffness coefficient G .

The concept presented in this Article is based on active control of the Young's modulus Y and the bending stiffness coefficient G of the glass shell by means of the attached piezoelectric Macro Fiber Composite (MFC) actuator. (Basic information on MFC properties

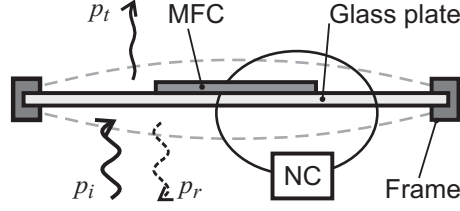


Figure 3: Scheme of the noise transmission suppression principle (cf. Fig. 1). The vibration amplitude normal to the surface of the glass plate is decreased using the effective stiffening of the piezoelectric Macro Fiber Composite (MFC) actuator due to the action of the active shunt circuit with a negative capacitance (NC);

can be found in [32].) The next Section presents a method for the active control of the Young's modulus Y and the bending stiffness coefficient G of the composite structure with piezoelectric layers.

IV. ACTIVE CONTROL OF YOUNG'S MODULUS AND BENDING STIFFNESS COEFFICIENT OF THE CURVED GLASS PLATE

Figure 3 shows the scheme of the noise transmission suppression principle, which is achieved using the reduction of the vibration amplitude normal to the surface of the glass plate due to the effective stiffening of the piezoelectric MFC actuator in the layered composite structure. The stiffening of the piezoelectric MFC actuator is realized using active shunt circuit with a negative capacitance (NC) according to the Active Elasticity Control method introduced by Date et al. [21]. The basic idea of the method is based on the superposition of direct and converse piezoelectric effects with Hooke's law: First, in-plane stress applied to elastic material produces strain according to Hooke's law. In the piezoelectric MFC actuator, the in-plane stress generates a charge on its electrodes due to the direct piezoelectric effect. The generated charge is introduced into the shunt circuit, which controls the electric voltage applied back to electrodes of the MFC actuator. The total strain of the MFC actuator is then equal to the sum of both: the stress-induced strain (due to Hooke's law) and the voltage-induced strain (due to the converse piezoelectric effect). When the voltage-induced strain cancels the stress-induced strain, the total strain of the MFC actuator equals zero even in nonzero stress applied to the MFC actuator. This actually means that the effective

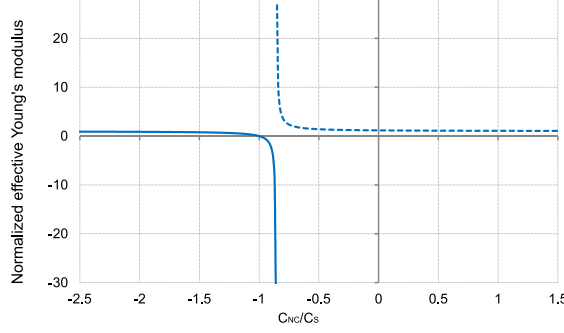


Figure 4: Normalized values of the effective Young's modulus Y_{MFC}/Y_S of the piezoelectric MFC actuator as a function of the shunt circuit capacitance C_{NC} normalized to the value of the MFC actuator static capacitance C_S . The values of Y_{MFC} are calculated using Eq. (10) for $k = 0.4$.

Young's modulus of the MFC actuator reaches infinity. The principle idea of the method can be simply expressed by the following formula for the effective value of Young's modulus:

$$Y_{\text{MFC}} = Y_S \left(1 + \frac{k^2}{1 - k^2 + \alpha} \right), \quad (10)$$

where Y_S is Young's modulus of piezoelectric MFC actuator material, k is the electromechanical coupling factor and $\alpha = C_{\text{NC}}/C_S$ is the ratio of the shunt circuit capacitance C_{NC} over the static capacitance C_S of the piezoelectric element.

Figure 4 shows the normalized values of the effective Young's modulus Y_{MFC}/Y_S of the piezoelectric MFC actuator as a function of the shunt circuit capacitance C_{NC} normalized to the value of the MFC actuator static capacitance C_S . The values of Y_{MFC} are calculated using Eq. (10) for $k = 0.4$. It follows from Eq. (10) that, when

$$C_{\text{NC}} = -(1 - k^2)C_S, \quad (11)$$

the effective Young's modulus reaches infinity. Such a situation has been profitably used in several noise suppression devices [22, 33–35].

Figure 5 shows the electrical scheme of the system, where the piezoelectric MFC actuator is shunted by the circuit that realizes negative values of capacitance. The shunt circuit with a negative capacitance is realized as a Negative Impedance Converter circuit (i.e. a one port circuit with an operational amplifier), where the reference impedance is realized as a capacitor C_0 connected in-series to the resistor R_0 . The effective value of the shunt circuit

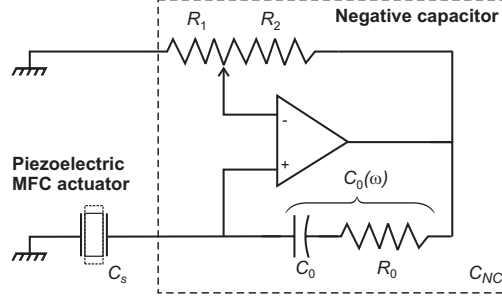


Figure 5: Electrical scheme of the piezoelectric MFC actuator shunted by the circuit that realizes negative values of effective capacitance. Symbol C_s stands for the piezoelectric element static capacitance, C_0 is the reference capacitance and R_0 and R_1 are tunable resistors.

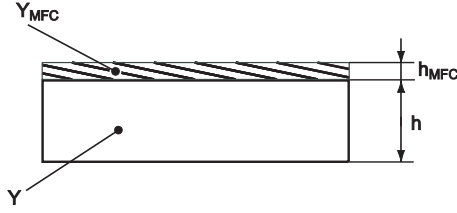


Figure 6: Cross-section of the layered composite structure, which consists of a glass plate of thickness h and an attached piezoelectric MFC actuator of thickness h_{MFC} .

capacitance is given by the formula:

$$C_{\text{NC}} = - \left(\frac{C_0}{1 + i\omega R_0 C_0} \right) \frac{R_2}{R_1}. \quad (12)$$

By proper adjustment of the tunable resistors R_0 and R_1 , the real and imaginary part of the shunt circuit effective capacitance can be adjusted in such a way that the condition given by Eq. (11) is satisfied and the effective Young's modulus of the MFC actuator is increased by several orders of magnitude.

Now, let us consider the composite structure of the glass plate and the attached MFC actuator with a cross-section shown in Fig. 6. Its effective Young's modulus Y_{Eff} is given by weighted average of the Young's moduli of the glass and the MFC, according to the formula:

$$Y_{\text{Eff}} = \frac{Yh + Y_{\text{MFC}}h_{\text{MFC}}}{h + h_{\text{MFC}}}, \quad (13)$$

where the symbols Y and Y_{MFC} stand for the Young's moduli of the glass and the MFC actuator, respectively. The symbols h and h_{MFC} stand for the thickness of the glass plate and MFC actuator, respectively.

The effective value of the bending stiffness coefficient G of the composite sandwich structure is given by the formula:

$$G_{\text{Eff}} = \frac{Y^2 h^4 + Y_{\text{MFC}}^2 h_{\text{MFC}}^4 + 2Y Y_{\text{MFC}} h h_{\text{MFC}} (2h^2 + 3h h_{\text{MFC}} + 2h_{\text{MFC}}^2)}{12(1 - \nu^2)(Yh + Y_{\text{MFC}} h_{\text{MFC}})}, \quad (14)$$

where ν is Poisson's ratio of the material. It is clearly seen that if Young's modulus of the MFC is increased using the effect of the shunt circuit, both effective values of the Young's modulus Y_{Eff} and the bending stiffness coefficient G_{Eff} of the composite sandwich structure are increased as well.

It is seen from Eqs. (7) and (9) that with an increase of the effective Young's modulus of the piezoelectric MFC actuator, the specific acoustic impedance of the curved glass shell increases. On the other hand, it should be pointed out that Eqs. (7) and (9) were calculated in a simplified model, where the values of curvature ξ , the effective Young's modulus Y_{Eff} and the bending stiffness coefficient G_{Eff} are constant. This is not the case of many applications of practical interest. In the next Section, there will be presented a Finite Element Method (FEM) model of a realistic system with a curved glass shell and 7 piezoelectric MFC actuators distributed on its surface. The FEM model of the system is then used for the analysis of its specific acoustic impedance.

V. FEM MODEL OF THE GLASS PLATE WITH THE ATTACHED SHUNTED MFC ACTUATOR

Figure 7 shows the geometry of the Finite Element Method (FEM) model of a curved glass shell with 7 attached MFC actuators. We consider a glass shell, which is fabricated by thermal bulging of the originally planar glass plate of thickness h and dimensions a and b . The presented configuration is selected in order to allow the suppression of majority of low-frequency vibrational modes. The vibrational response of the curved glass shell expressed by the displacement vector u_i is governed by the equations of motion on the form:

$$2\rho \frac{\partial^2 u_i}{\partial t^2} - \nabla_j [c_{ijkl} (\nabla_k u_l + \nabla_l u_k)] = 0, \quad (15)$$

where ρ is the mass density of glass, c_{ijkl} are the components of elastic stiffness tensor, and $\nabla_i = \partial/\partial x_i$ is the i -th component of the gradient operator. Since we are interested in the steady-state vibrational response of the curved glass shell, we consider the harmonic

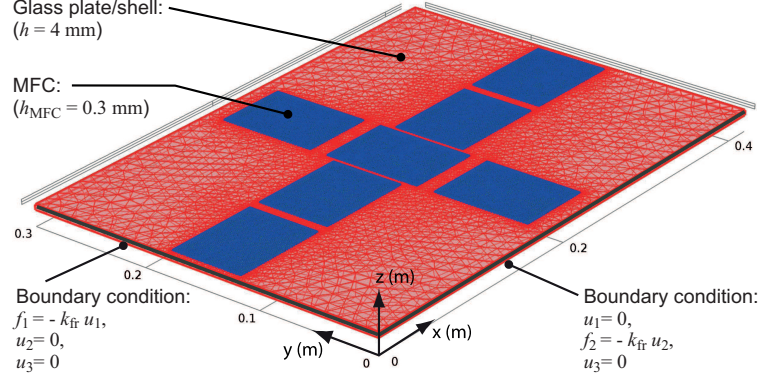


Figure 7: Geometry of the Finite Element Method (FEM) model of a curved glass shell with 7 attached MFC actuators. The presented configuration is selected in order to allow the suppression of majority of low-frequency vibrational modes. The considered coordinate system and boundary conditions are indicated.

time dependence of the displacement vector, i.e. $u_i(x, y, z, t) = u_i(x, y, z) e^{i\omega t}$, and the equations of motion Eq. (15) can be written in the form:

$$2\omega^2 \varrho u_i + \nabla_j [c_{ijkl} (\nabla_k u_l + \nabla_l u_k)] = 0, \quad (16)$$

In our study, the same governing equations can be also applied to describe the vibrational response of the MFC actuators, however, with the frequency dependent values of the components of elastic stiffness tensor. Justification for such a simplification is as follows. Since the MFC actuator consists of the piezoelectric fibers embedded in an epoxy matrix, connected to interdigital electrodes, and laminated in thin kapton layers, one can expect that detailed vibration of such a complicated composite structure is difficult to model in full detail. On the other hand, the MFC actuator operates as d_{31} -type piezoelectric actuator with some macroscopic values of piezoelectric coefficients. In the same manner, one can introduce the effect of the shunt circuit on the lines of derivation of Eq. (10) presented in [21]. As it has been written above, the effective value of Young's modulus of the shunted MFC actuator is a function of the ratio of the shunt capacitance C_{NC} over the static capacitance C_S of the actuator. Since the capacitance of the negative capacitor is frequency-dependent, as it is seen in Eq. (12), the matching of capacitances C_{NC} and C_S according to the condition expressed by Eq. (11) required for obtaining large effective values of Young's modulus can be obtained only in a relatively narrow frequency range due to virtually constant value of the capacitance C_S .

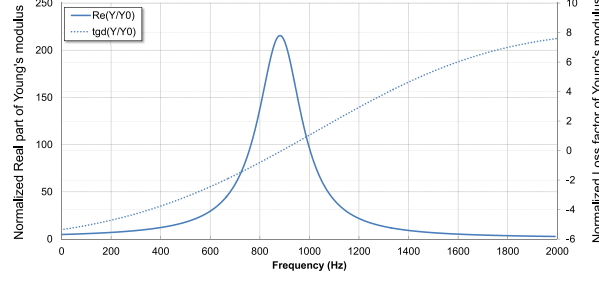


Figure 8: Effective value of the normalized real part and loss factor of Young's modulus of MFC actuator with shunted active NC circuit. Proper adjustment of the NC circuit could increase the value of Young's modulus by a factor of 200. The frequency 890 Hz of the peak values of the real part of Young's modulus is adjusted to the frequency of a particular resonant mode of the glass plate.

The frequency dependence of the effective Young's modulus of the MFC actuator shunted by the negative capacitor was analyzed in detail in the recent work by Nováková and Mokřý [36]. Figure 8 presents the typical frequency dependence of the real part and the loss tangent of the effective value of Young's modulus in a broad frequency range. The frequency 890 Hz of the peak values of the real part of Young's modulus is adjusted to the frequency of a particular resonant mode of the glass plate via the particular values of the circuit parameters of the negative capacitor. In our simulations, we have therefore considered the $c_{1111} = Y_{\text{MFC}}(\omega)$ and $c_{2222} = Y_{\text{MFC}}(\omega)$ components of the elastic stiffness tensor of the MFC actuator as being frequency dependent according to the function presented in Fig. 8.

Further we consider that the glass shell with MFC actuators interacts with the acoustic field in the air above and below the shell. We consider a sound source that produces a plane incident wave below the glass shell:

$$p_i(z, t) = P_i e^{i(\omega t - kz)}, \quad (17)$$

where k is the length of the wave vector of the incident sound wave, which is oriented along the z -axis. The acoustic pressure p distribution in the air above and below the glass shell is governed by the following equation:

$$\frac{1}{\rho_0 c^2} \frac{\partial^2 p}{\partial t^2} + \nabla_i \left(-\frac{1}{\rho_0} \nabla_i p \right) = 0, \quad (18)$$

where ϱ_0 and c stand for the mass density and the sound speed in the air. Again, we are interested in the steady-state distribution of the acoustic pressure, i.e. $p(x, y, z, t) = p(x, y, z) e^{i\omega t}$, and the equation above reduces down to the form:

$$-\frac{\omega^2 p}{\rho_0 c^2} + \nabla_i \left(-\frac{1}{\rho_0} \nabla_i p \right) = 0. \quad (19)$$

It should be noted that below the glass shell the acoustic pressure is given by the sum of the acoustic pressures of the incident and reflected sound waves, i.e. $p = p_i + p_r$. Above the glass shell, the acoustic pressure is equal to the acoustic pressure of the transmitted sound wave, i.e. $p = p_t$.

The calculation of the transmission loss is based on analysis of the interaction between the vibrating glass shell and the surrounding air. In order to proceed the calculation, the system of partial differential equations Eqs. (16) and (19) should be appended by the system in boundary and internal boundary conditions: First, the acoustic pressure exerts the force on the glass shell at its interface with the air, which can be expressed by the following internal boundary condition:

$$n_j [c_{ijkl} (\nabla_k u_l + \nabla_l u_k)] = 2n_i p, \quad (20)$$

where n_i is the i -th component of the outward-pointing (seen from the inside of the glass shell) unit vector normal to the surface of the glass shell with the MFC actuators. Second, the normal accelerations of the glass surface and the air particles are equal at the interfaces of the glass shell and the air:

$$\omega^2 (n_i u_i) = n_i (1/\varrho_0) \nabla_i p. \quad (21)$$

Finally, it will be presented later in this Article that a special attention must be paid to boundary conditions for the displacement u_i at the edges, where the glass shell is clamped at the frame. In many real situations, the glass shell is not ideally fixed and the frame that clamps the glass shell is somehow flexible. In order to take this effect into account, we approximated the boundary condition by considering a reaction force \mathbf{f}_{fr} from the spring system of the frame as being proportional to the frontal displacement of the glass shell with respect to the frame, i.e. $\mathbf{f}_{\text{fr}} = -k_{\text{fr}} \mathbf{u}$, where the symbol k_{fr} stands for the effective spring constant of the frame, which can be estimated from geometrical parameters and Young's

moduli of the frame. This yields the following boundary conditions:

$$f_1 = c_{11kl} (\nabla_k u_l + \nabla_l u_k) = -k_{\text{fr}} u_1, \quad (22a)$$

$$u_2 = 0, \quad (22b)$$

$$u_3 = 0 \quad (22c)$$

on the glass edges where $x = 0$ and $x = a$ and

$$u_1 = 0, \quad (23a)$$

$$f_2 = c_{22kl} (\nabla_k u_l + \nabla_l u_k) = -k_{\text{fr}} u_2, \quad (23b)$$

$$u_3 = 0 \quad (23c)$$

for $y = 0$ and $y = b$. It should be noted that the boundary conditions given by Eqs. (22) and (23) express the limited ability of the frame to keep the glass shell edge at the same position during the vibration movements. As a result, the glass shell movements acquire some properties typical for membranes, which yield the shift of the resonant frequencies to lower values.

The boundary problem for partial differential equations given by Eqs. (16), (19)-(23) was solved using COMSOL Multiphysics software. The solution yields spatial distributions of the acoustic pressure p and the glass shell displacements u_i . Then, the specific acoustic impedance of the glass shell Z_w was estimated for every frequency ω of the incident sound wave using the following approximative formula:

$$Z_w(\omega) \approx \frac{\Delta P(\omega)}{i\omega W(\omega)}, \quad (24)$$

where ΔP is the amplitude of the acoustic pressure difference above and below the middle point of the glass shell, W is the amplitude of the normal displacement at the middle point of the glass shell. The acoustic TL was obtained using Eq. (2).

Numerical predictions of the FEM model should be compared with experimental data. The next Section presents a simple setup for obtaining experimental data.

VI. EXPERIMENTAL SETUP FOR THE ACOUSTIC TRANSMISSION LOSS MEASUREMENTS

Figure 9 shows the experimental setup for the approximative measurements of the specific acoustic impedance. The glass plate is clamped in a wooden frame of the inner dimensions

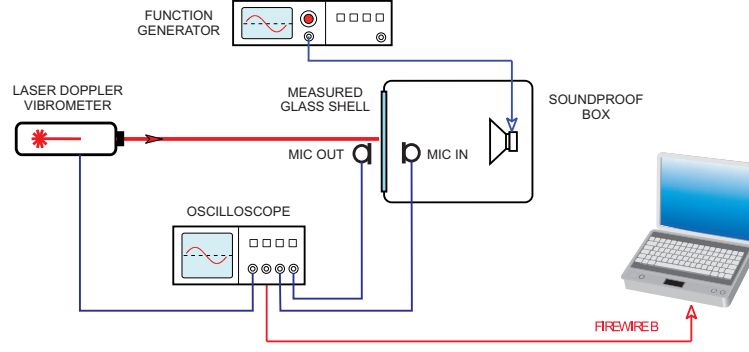


Figure 9: Experimental setup for the approximative measurements of the specific acoustic impedance. The glass plate is clamped in a wooden frame and forms a lid of the soundproof box with a loudspeaker. The microphone IN inside the acoustic box and the microphone OUT out of the wooden box measures the difference of acoustic pressures Δp at the opposite sides of the glass plate. Laser Doppler vibrometer measures the amplitude of the vibration velocity V of the glass plate middle point. The specific acoustic impedance Z_w is approximated by the ratio $\Delta p/V$ and the value of the acoustic TL is estimated using Eq. (2).

0.42×0.3 m. This structure forms a lid of the soundproof box with a loudspeaker that produces the source of the incident sound wave. The microphone IN inside the box and the microphone OUT out of the wooden box measures the difference of acoustic pressures Δp at the opposite sides of the glass plate. They are placed approximately 1 cm above and below the middle point of the glass plate. Laser Doppler vibrometer measures the amplitude of the vibration velocity V of the glass plate middle point. The specific acoustic impedance Z_w is approximated by the ratio $\Delta p/V$ and the value of the acoustic TL is estimated using Eq. (2).

Using such a measurement setup, only an approximative value of the TL can be obtained because of limited dimensions of the box. However, it is acceptable for the demonstration of the noise suppression efficiency. The next section presents the numerical results of our FEM model simulations and their comparison with the approximative experimental data.

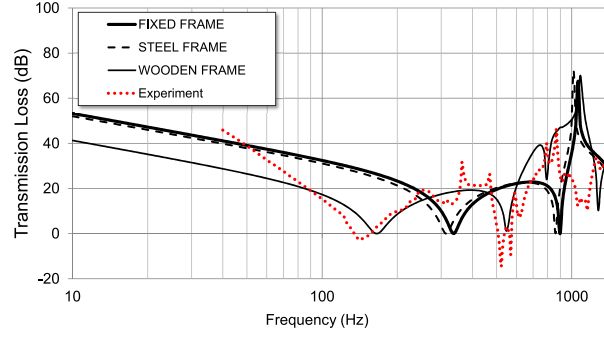


Figure 10: Comparison of the approximative measurement of the frequency dependency of the acoustic transmission loss through the planar glass plate (dotted) with the FEM model predictions for three different boundary conditions: Ideally fixed glass (solid thick), steel frame with $k_{fr} = 1 \cdot 10^{10} \text{ N}\cdot\text{m}^{-1}$ (dashed thin), wooden frame with $k_{fr} = 1 \cdot 10^7 \text{ N}\cdot\text{m}^{-1}$ (solid thin). An acceptable agreement of the experimental data with the wooden flexible frame is noticeable.

VII. RESULTS OF THE FEM MODEL SIMULATIONS AND THE EXPERIMENTAL VERIFICATION

Figure 10 shows the frequency dependencies of the acoustic TL obtained from the FEM model simulations. Following numerical parameters were considered in the numerical simulations: $P_i = 0.2 \text{ Pa}$ that corresponds to 80 dB of the sound pressure level, $a = 0.42\text{m}$, $b = 0.3\text{m}$, $h = 4\text{mm}$. The Young's modulus of the glass $73.1 \cdot 10^9 \text{ Pa}$, the Poisson's ratio of the glass 0.17 and the mass density of the glass $2203 \text{ kg}\cdot\text{m}^{-3}$. Young's modulus of the electrically opened piezoelectric MFC actuator is equal to $Y_S = 30.4 \cdot 10^9 \text{ Pa}$. Three situations with different boundary conditions of the glass plate were considered: Ideally fixed glass (solid thick), steel frame with $k_{fr} = 1 \cdot 10^{10} \text{ N}\cdot\text{m}^{-1}$ (dashed thin), wooden frame with $k_{fr} = 1 \cdot 10^7 \text{ N}\cdot\text{m}^{-1}$ (solid thin). It is seen that steel frame represents a very good approximation of the ideally fixed glass plate. On the other hand, the smaller value (by 3 orders of magnitude) of the effective spring constant of the frame causes a reasonable decrease in the resonant frequencies of the resonant modes of the glass plate. An acceptable agreement of the experimental data with the wooden flexible frame is noticeable. The acquired agreement of the FEM model prediction with the approximative experimental data indicates that the developed FEM model is credible and that it may serve valuable predictions of the effect of piezoelectric MFC actuators shunted by negative capacitance circuits on the frequency

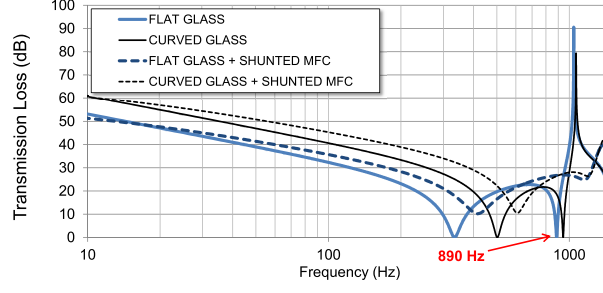


Figure 11: Frequency dependencies of the acoustic TL obtained from the FEM model simulations. Parameters of the curves are the curvatures and the electrical conditions of the piezoelectric MFC actuators: Planar glass plate with opened MFC actuator (solid thick), bulged glass shell with opened MFC actuator (solid thin), planar glass plate with the MFC actuator shunted by NC circuit (dashed thick), and bulged glass shell with the MFC actuator shunted by NC circuit (dashed thin). The appreciable increase in the acoustic transmission loss by 10 – 25 dB in the frequency range below 400 Hz due to the small increase in the curvature of the glass shell is noticeable. In addition, the FEM model predictions indicate that it is possible to further improve the TL by about 15 dB by the effect of the shunt NC circuit.

dependence of the acoustic transmission loss.

Figure 11 shows frequency dependence of the acoustic TL obtained from FEM model simulations. Four situations with different curvatures and the electrical conditions of the piezoelectric MFC actuators were considered: Planar glass plate with opened MFC actuator (solid thick), bulged glass shell with opened MFC actuator (solid thin), planar glass plate with the MFC actuator shunted by NC circuit (dashed thick), and bulged glass shell with the MFC actuator shunted by NC circuit (dashed thin). The fixed boundary conditions at the edges of the glass shell are considered, i.e. $u_i = 0$. The bulged shape of the glass shell was approximated using the displacement function in the z -axis direction in the form $z_{\max} \sin(\pi x/a) \sin(\pi y/b)$, where $z_{\max} = 5$ mm.

It is presented in Fig. 8 that it is possible to increase the effective value of the Young's modulus by a factor of 100 in the frequency range from 0.75 kHz to 1 kHz and by a factor of 200 in a narrow frequency range around 0.89 kHz using the shunt circuit with a negative capacitance. Figure 11 shows that such an increase in the effective value of the Young's modulus of the MFC actuators has an appreciable effect on the frequency dependence of

the acoustic TL through the glass shell. The numerical predictions of the FEM model indicate that it is possible increase the acoustic transmission loss by 20 dB and 25 dB at the frequencies of the first and second resonant modes of the planar and curved glass shells, respectively.

VIII. CONCLUSIONS

We have analyzed the possibility to increase the acoustic transmission loss of sound transmitted through the planar or curved glass shells using the attached piezoelectric MFC actuators shunted by the active circuits with a negative capacitance.

The analytical approximative model of the sound transmission through the rectangular spherically curved laminar composite shell is developed. The analytical model was used to determine the most important features that control the sound transmission through the shell: radius of curvature, Young's modulus, and the bending stiffness coefficient of the shell. The method for the active control of the Young's modulus and the bending stiffness coefficient of the composite sandwich structure that consists of a glass plate and the attached piezoelectric MFC actuator is presented. Since the analytical model is applicable only to situations of not much practical interest, the FEM model of curved glass shell with attached piezoelectric MFC actuators shunted by circuits with a negative capacitance has been developed. The effect of the flexible frame that clamps the glass shell edges was taken into account. The experimental setup for the approximative measurements of the specific acoustic impedance is presented.

The predictions of the acoustic transmission loss frequency dependencies obtained by the FEM model show a good agreement with the approximative measurements. It was shown that a special attention must be paid to the specification of the correct boundary conditions at the edges of the glass shell. Analysis of the effect of the active elasticity control on the acoustic transmission loss of sound has been performed using the FEM model. The results indicated that it is possible increase the acoustic transmission loss by 20 dB and 25 dB at the frequencies of the first and second resonant modes of the planar and curved glass shells, respectively, using the effect of the shunt circuit with a negative capacitance.

All in all, the Article presents a promising approach for the suppression of the noise transmission through glass plates and shells using piezoelectric MFC actuators and negative

capacitance circuits. The method starts from the vibrational analysis focusing on the effects of the elastic properties of the composite structure with piezoelectric layers. Using active shunt circuits with a negative capacitance, the effective elastic properties of the piezoelectric layers can be controlled to a large extent. As a result, the appreciable increase in the acoustic transmission loss through the glass shell composite can be achieved. The advantages of this method stem from its generality and simplicity offering an efficient tool for the control of the noise transmission through glass windows especially in the low-frequency range where the passive methods are ineffective.

Acknowledgment

This work was supported by Czech Science Foundation Project No.: GACR 101/08/1279, co-financed from the student grant SGS 2012/7821 Interactive Mechatronics Systems Using the Cybernetics Principles, and the European Regional Development Fund and the Ministry of Education, Youth and Sports of the Czech Republic in the Project No. CZ.1.05/2.1.00/03.0079: Research Center for Special Optics and Optoelectronic Systems (TOPTEC).

-
- [1] F. Fahy, *Foundations of engineering acoustics*. Academic Press, 2001.
 - [2] C. Fuller, “Active control of sound-transmission radiation from elastic plates by vibration inputs .1. analysis,” *Journal Of Sound And Vibration*, vol. 136, pp. 1–15, JAN 8 1990.
 - [3] V. Metcalf, C. Fuller, R. Silcox, and D. Brown, “Active control of sound-transmission radiation from elastic plates by vibration inputs .2. experiments,” *Journal Of Sound And Vibration*, vol. 153, pp. 387–402, MAR 22 1992.
 - [4] B. Wang, C. Fuller, and E. Dimitriadis, “Active control of noise transmission through rectangular-plates using multiple piezoelectric or point force actuators,” *Journal Of The Acoustical Society Of America*, vol. 90, pp. 2820–2830, NOV 1991.
 - [5] H. Zhu, X. Yu, R. Rajamani, and K. Stelson, “Active control of glass panels for reduction of sound transmission through windows,” *Mechatronics*, vol. 14, pp. 805–819, SEP 2004.
 - [6] A. Jakob and M. Moser, “Active control of double-glazed windows - Part I: Feedforward

- control,” *Applied Acoustics*, vol. 64, pp. 163–182, FEB 2003.
- [7] A. Jakob and M. Moser, “Active control of double-glazed windows. Part II: Feedback control,” *Applied Acoustics*, vol. 64, pp. 183–196, FEB 2003.
 - [8] J. Pan, C. Hansen, and D. Bies, “Active control of noise transmission through a panel into a cavity .1. analytical study,” *Journal Of The Acoustical Society Of America*, vol. 87, pp. 2098–2108, MAY 1990.
 - [9] J. Pan and C. Hansen, “Active control of noise transmission through a panel into a cavity .2. experimental-study,” *Journal Of The Acoustical Society Of America*, vol. 90, pp. 1488–1492, SEP 1991.
 - [10] S. Hirsch and J. Sun, “Numerical studies of acoustic boundary control for interior sound suppression,” *Journal Of The Acoustical Society Of America*, vol. 104, pp. 2227–2235, OCT 1998.
 - [11] J. Carneal and C. Fuller, “An analytical and experimental investigation of active structural acoustic control of noise transmission through double panel systems,” *Journal Of Sound And Vibration*, vol. 272, pp. 749–771, MAY 6 2004.
 - [12] B. Naticchia and A. Carbonari, “Feasibility analysis of an active technology to improve acoustic comfort in buildings,” *Building And Environment*, vol. 42, pp. 2785–2796, JUL 2007.
 - [13] Q. Mao and S. Pietrzko, “Control of sound transmission through double wall partitions using optimally tuned Helmholtz resonators,” *Acta Acustica United With Acustica*, vol. 91, pp. 723–731, JUL-AUG 2005.
 - [14] Q. Mao and S. Pietrzko, “Experimental study for control of sound transmission through double glazed window using optimally tuned Helmholtz resonators,” *Applied Acoustics*, vol. 71, pp. 32–38, JAN 2010.
 - [15] S. J. Pietrzko and Q. Mao, “New results in active and passive control of sound transmission through double wall structures,” *Aerospace Science And Technology*, vol. 12, pp. 42–53, JAN 2008.
 - [16] S. Behrens, A. Fleming, and S. Moheimani, “A broadband controller for shunt piezoelectric damping of structural vibration,” *Smart Materials & Structures*, vol. 12, pp. 18–28, Feb 2003.
 - [17] A. Fleming, S. Behrens, and S. Moheimani, “Optimization and implementation of multimode piezoelectric shunt damping systems,” *IEEE-ASME Transactions On Mechatronics*, vol. 7, pp. 87–94, MAR 2002.

- [18] A. Belloli, D. Niederberger, S. Pietrzko, M. Morari, and P. Ermanni, “Structural vibration control via R-L shunted active fiber composites,” *Journal Of Intelligent Material Systems And Structures*, vol. 18, pp. 275–287, Mar 2007. 15th International Conference on Adaptive Structures and Technologies (ICAST), Bar Harbor, ME, OCT 24-27, 2004.
- [19] J. Q. Ming Yuan, Hongli Ji and T. Ma, “Active control of sound transmission through a stiffened panel using a hybrid control strategy,” *Journal of Intelligent Material Systems and Structures*, vol. 23, pp. 791–803, 2012.
- [20] M. Ciminello, L. Lecce, S. Ameduri, A. Calabro, and A. Concilio, “Multi-tone Switching Shunt Control by a PZT Network Embedded into a Fiberglass Panel: Design, Manufacture, and Test,” *Journal Of Intelligent Material Systems And Structures*, vol. 21, pp. 437–451, MAR 2010.
- [21] M. Date, M. Kutani, and S. Sakai, “Electrically controlled elasticity utilizing piezoelectric coupling,” *Journal of Applied Physics*, vol. 87, no. 2, pp. 863–868, 2000. NIC.
- [22] H. Kodama, T. Okubo, M. Date, and E. Fukada, “Sound reflection and absorption by piezoelectric polymer films,” in *Proc. Materials Research Society Symposium*, vol. 698, (506 Keystone Drive, Warrendale, PA 15088-7563 USA), pp. 43–52, Materials Research Society, 2002. Symposium on Rapid Prototyping Technologies-From Tissue Engineering to Conformal Electronics held at the 2001 MRS Fall Meeting, BOSTON, MA, NOV 28-30, 2001.
- [23] E. Fukada, M. Date, K. Kimura, T. Okubo, H. Kodama, P. Mokry, and K. Yamamoto, “Sound isolation by piezoelectric polymer films connected to negative capacitance circuits,” *IEEE Transactions on Dielectrics and Electrical Insulation*, vol. 11, pp. 328–333, APR 2004.
- [24] K. Yamamoto, K. Kimura, T. Okubo, H. Kodama, M. Date, and E. Fukada, “Control of low frequency sound insulation by curved polymer films,” in *Proc. Inter-noise 2005*, 2005.
- [25] K. Imoto, M. Nishiura, K. Yamamoto, M. Date, E. Fukada, and Y. Tajitsu, “Elasticity control of piezoelectric lead zirconate titanate (pzt) materials using negative-capacitance circuits,” *Japanese Journal of Applied Physics*, vol. 44, no. 9B, pp. 7019–7023, 2005.
- [26] K. Tahara, H. Ueda, J. Takarada, K. Imoto, K. Yamamoto, M. Date, E. Fukada, and Y. Tajitsu, “Basic study of application for elasticity control of piezoelectric lead zirconate titanate materials using negative-capacitance circuits to sound shielding technology,” *Japanese Journal of Applied Physics*, vol. 45, no. 9B, pp. 7422–7425, 2006.
- [27] J. Václavík and P. Mokřý, “Measurement of mechanical and electrical energy flows in the

- semiactive piezoelectric shunt damping system,” *Journal of Intelligent Material Systems and Structures*, vol. 23, pp. 527–533, 2012.
- [28] Z. Maekawa and P. Lord, *Environmental and Architectural Acoustics*. Taylor & Francis, 1994.
- [29] W. Soedel, *Vibrations of Shells and Plates*. Marcel Dekker, 2004.
- [30] K. Graff, *Wave motion in elastic solids*. Dover Publication, 1991.
- [31] S. Timoshenko, *Theory of Plates and Shells*. McGraw-Hill Book Company, 1940.
- [32] W. Wilkie, R. Bryant, J. High, R. Fox, R. Hellbaum, A. Jalink, B. Little, and P. Mirick, “Low-cost piezocomposite actuator for structural control applications,” in *Smart Structures And Material 2000: Industrial And Commercial Applications Of Smart Structures Technologies* (Jacobs, JH, ed.), vol. 3991 of *Proceedings Of The Society Of Photo-optical Instrumentation Engineers (spie)*, pp. 323–334, SPIE; Soc Exptl Mech; Amer Soc Mech Engn; BFGoodrich; Def Adv Res Projects Agcy; USA Res Off; USAF Res Lab; Ceram Soc Japan; Intelligent Mat Forum, Japan, 2000. Smart Structures and Materials 2000 Conference, NEWPORT BEACH, CA, MAR 05-09, 2000.
- [33] T. Okubo, H. Kodama, K. Kimura, K. Yamamoto, E. Fukada, and M. Date, “Sound-isolation and vibration-isolating efficiency piezoelectric materials connected to negative capacitance circuits,” in *Proc. 17th International Congress on Acoustics*, pp. 301–306, 2001.
- [34] P. Mokřý, E. Fukada, and K. Yamamoto, “Noise shielding system utilizing a thin piezoelectric membrane and elasticity control,” *Journal of Applied Physics*, vol. 94, no. 1, pp. 789–796, 2003.
- [35] T. S. Sluka, H. Kodama, E. Fukada, and P. Mokřý, “Sound shielding by a piezoelectric membrane and a negative capacitor with feedback control,” *IEEE Transactions on Ultrasonics, Ferroelectrics, and Frequency Control*, vol. 55, pp. 1859–1866, AUG 2008.
- [36] K. Novakova and P. Mokry, “Numerical simulation of mechanical behavior of a macro fiber composite piezoelectric actuator shunted by a negative capacitor,” in *Electronics, Control, Measurement and Signals (ECMS), 2011 10th International Workshop on*, 2011.